A Membrane-Reconstituted Multisubunit Functional Proton Pump on Mesoporous Silica Particles

Gustav Nordlund,[†] Jovice Boon Sing Ng,[‡] Lennart Bergström,[‡] and Peter Brzezinski[†,*]

[†]Department of Biochemistry and Biophysics, Centre for Biomembrane Research, Stockholm University, SE-10691 Stockholm, Sweden, and [‡]Materials Chemistry Research Group, Department of Physical, Inorganic and Structural Chemistry, Stockholm University, SE-10691 Stockholm, Sweden

ABSTRACT We have investigated formation of a proteolipid membrane surrounding mesoporous silica particles with a diameter of 550 nm and pore sizes of 3.0 nm. A multisubunit redox-driven proton pump, cytochrome *c* oxidase, was incorporated into the membrane, and we show that the enzyme is functional, both with respect to catalysis of O_2 reduction to water, and charge separation across the membrane. The orientation of cytochrome *c* oxidase in the membrane was found to be the same (~70%) in the lipid vesicles and in the silica-particle-supported lipid membrane, which provides information on the mechanism by which the vesicles adsorb to the surface. Furthermore, cytochrome *c* oxidase could maintain a proton electrochemical gradient across the supported proteomembrane, that is, the membrane system was proton tight, defining an interior particle compartment that is separated from the surrounding aqueous media. Such a biofunctional cellular interface, supported onto a colloid that has a connected interior cytoskeleton-like pore structure, provides a basis for functional studies of membrane-bound transport proteins, and also for applications within pharmaceutical drug delivery.

KEYWORDS: supported lipid bilayer · mesoporous spheres · nanoparticles · membrane protein · drug delivery · cytochrome *c* oxidase

Recent developments in the synthesis of self-assembled materials have made it possible to design and manufacture surfactant-templated mesoporous silica particles with stable mesostructure, narrow pore size distribution, adjustable pore size, pore connectivity, and morphology.[1−5] The accessible surface area and pore volume of these particles are typically very large, making it possible to use them as vehicles for controlled delivery of, for example, drugs and genes.[6−8] The internal and external surfaces of the mesoporous material can be modified to immobilize and control the release of, for example, anticancer drugs.[9−11] Recent works have shown how coumarin, quantum dots, and other molecules can open and close the pores triggering release of specific molecules.[12−14] Durable encapsulation of the molecules can also be accomplished by deposition of a lipid membrane, which covers the entire surface of the particle.[15−22] The release of these molecules could be mediated by specific channels or transporters incorporated into the membrane, which requires development of methodology and techniques for incorporation of integral membrane proteins into the particle-supported lipid layers. Such protein−membrane particle systems are also of significant interest for functional studies of membrane proteins because they provide a robust system for mechanistic investigations of transport mechanisms. Indeed, recent reports describe successful incorporation of a number of simple and structurally stable membrane proteins, such as bacteriorhodopsin, into supported membranes onto solid[20] and porous[23] silica particles. In the present study, we have used a multisubunit, transmembrane complex "molecular machine", cytochrome *c* oxidase (CytcO, cytochrome aa_3) from *Rhodobacter sphaeroides*. In earlier studies methods have been developed to adsorb membrane-reconstituted CytcO at planar solid surfaces.[24−27] Here, we demonstrate that CytcO can be incorporated into a lipid membrane supported onto the outer surface of cell-mimetic mesoporous silica colloids with an interior water-filled volume. The mesoporous silica particles are monodisperse spheres with a diameter of 550 nm and pore-size of 3.0 nm, prepared by a modified Stoeber method using hexadecyltrimethyl ammonium bromide as the templating molecule.[28]

The enzyme CytcO is a proton pump that is driven by electron transfer from cytochrome *c* to oxygen, which is reduced to water. Cytochrome *c* initially donates electrons to a copper site (Cu_A), located within subunit II near the positive side (see later) of the membrane. The electrons are then transferred consecutively to a heme group

*Address correspondence to peterb@dbb.su.se.

Received for review May 26, 2009 and accepted July 28, 2009.

Published online August 4, 2009.
10.1021/nn9005413 CCC: $40.75

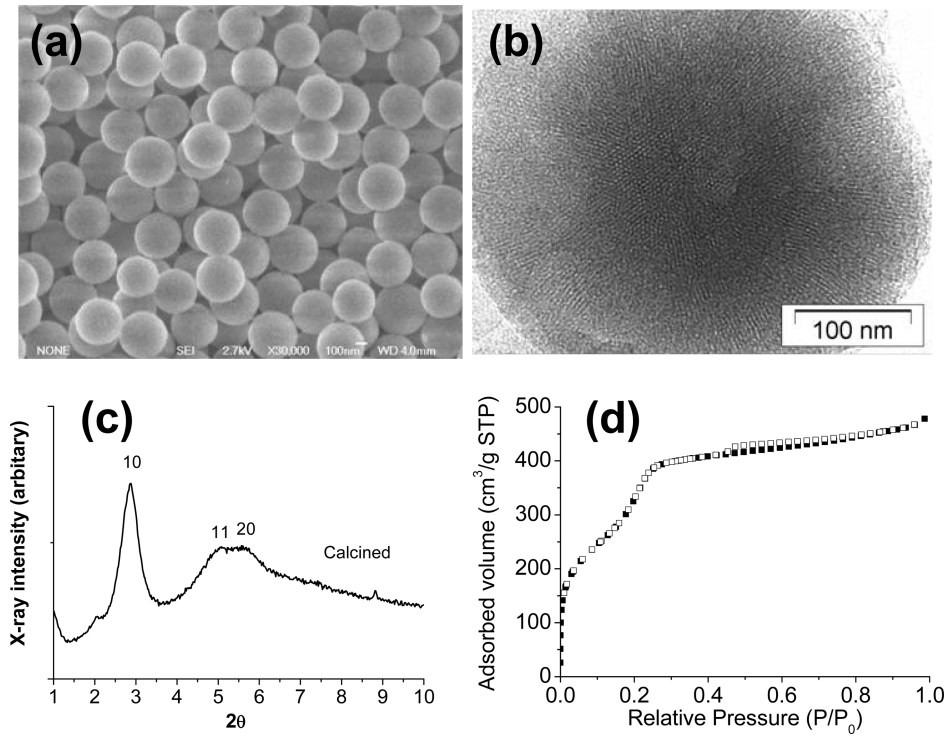

Figure 1. Characterization of the calcined mesoporous silica particles. (a) A scanning electron micrograph reveals the spherical morphology and monodispersity of the particles. (b) Thin microtomed equatorial slice of the particles viewed under transmission electron microscope exhibits pore channels extending radially from the core to the sphere surface. (c) The particles exhibit an X-ray diffraction of a 2D hexagonal mesostructure having a sharp 10 peak, with the higher order 11 and 20 peaks merged together. (d) The nitrogen sorption isotherm can be classified as type IV isotherms according to the IUPAC nomenclature, which is typically observed for 2D hexagonal mesoporous structures.[1]

(heme *a*) and then to the catalytic site, which consists of another heme group, called heme a_3, and a copper ion (Cu_B) in close vicinity. When the catalytic site is reduced, heme a_3 binds O_2, which is then reduced to water accompanied by proton uptake from the negative side of the membrane. Because electrons are donated from one side (the positive side) of the membrane, while protons are taken up from the opposite side (the negative side, inside of the bacterial cell), the reaction catalyzed by CytcO results in a charge separation across the membrane, which is equivalent to moving a positive charge from the negative to the positive side of the membrane. In addition, the reaction catalyzed by CytcO is linked to pumping of one proton across the membrane for each electron transferred from cytochrome *c* to O_2, thereby increasing the overall charge translocation stoichiometry making it equivalent to translocation of two positive charges per electron transferred to the catalytic site.

The advantage of using CytcO to study proteomembrane formation at solid particles is that the protein has a well-defined optical absorption spectrum, which is dependent on, for example, ligand binding to the catalytic site. Furthermore, the protein can be selectively reduced, either only from one or from both sides of the membrane, providing a simple way to determine protein orientation without the use of external labels. Furthermore, the capacity of the membrane to hold a transmembrane proton electrochemical gradient, which reflects the integrity of the membrane, can be assessed because the CytcO turnover rate is dependent on the membrane potential. The orientation of CytcO in the lipid vesicles was found to be preserved in the silica-particle supported lipid membrane after the vesicle fusion event. This finding allows us to speculate about the mechanisms by which the vesicles adsorbed, ruptured, and fused at the silica particle surface. The CytcO incorporated into the supported membrane was active and did not display any structural changes around the catalytic site. The CytcO-containing lipid membrane supported by the mesoporous silica particles was sufficiently proton tight to allow for build-up of a proton electrochemical gradient between the closed compartment within the particles and the surrounding solution.

RESULTS AND DISCUSSION

The calcined particles are monodispersed spheres with an average particle size of 550 ± 30 nm (Figure 1a). Their thin microtomed equatorial slices revealed bundles of hexagonally ordered cylindrical channels that extend radially from the sphere core to the surface (Figure 1b). The X-ray diffraction spectra (Figure 1c) exhibit diffraction peaks of an ordered 2-D hexagonal mesopore structure. Nitrogen sorption measurements (Figure 1d) showed that the particles have a pore size of 3.0 nm, a specific area of 1280 $m^2\ g^{-1}$, and pore

volume of 0.88 $cm^3\ g^{-1}$. Results from previous studies have shown that the pores are oriented perpendicular to the external surface.[28] The density, ρ_1, of the mesoporous particles is estimated as follow:

$$\rho_1 = \frac{1}{\frac{1}{\rho_{SiO_2}} + V_{pore}} \quad (1)$$

where V_{pore} is the pore volume per unit weight. Assuming that the density of amorphous silica is 2.2 g/cm^3, and the estimated pore volume is 0.88 cm^3/g (from the nitrogen isotherm), ρ_1 is 0.75 g/cm^3. This particle density corresponds to an estimated exterior surface area of 14.6 m^2/g ($\rho_1^{-1}A/V$, where ρ_1 is the particle density, A is the area and V is the volume), that is, the ratio of the interior and exterior surface area is ~90.

CytcO was reconstituted into the small unilamellar vesicles, and these CytcO-containing vesicles were subsequently used to cover the mesoporous silica particles. The fluorescence from the CytcO-containing vesicles (i) with fluorescein-labeled lipids added, (ii) with maleimide-fluorescein-labeled CytcO, or (iii) with fluorescein trapped within, was analyzed before (using a Fluorometer) and after (using flow cytometry) interaction with the silica particles.[29] The data show that the relative fluorescence values for vesicles with (i) fluorescein-labeled lipids and for (ii) fluorescein-labeled CytcO were approximately the same before and after reaction with the particles (Table 1). Because the light scattering intensity depends strongly on particle size, the flow cytometer only detects the mesoporous silica particles and not the much smaller vesicles. Hence, these measurements show that the CytcO-vesicles were adsorbed onto the surface of the particles and that the ratio of fluorescence values originating from pure lipids and from fluorescein-labeled CytcO was the same for the vesicle sample and after adsorption to particles. In other words, the data indicate that the protein−lipid ratio was the same in the vesicles and in the CytcO-membrane at the particle surface.

TABLE 1. Relative Fluorescence Values of Vesicles and Membrane-Covered Particles[a]

	Flu-lipids (i)	Flu-CytcO (ii)	Flu inside/Flu-lipids[b] (iii)
vesicles	93%	7%	10
particles	91%	9%	0.12

[a]The relative fluorescence values obtained with (i) fluorescein-labeled lipids (Flu-lipids), (ii) fluorescein-labeled CytcO (Flu-CytcO) in vesicles and (iii) the ratio of fluorescence values obtained from measurements with fluorescein entrapped within vesicles and fluorescein-labeled lipids.[29] These values are shown for vesicles only ("vesicles") and after deposition of the membrane on the silica particle surface ("particles"). The measurements were done using a fluorometer (for vesicles only) or a flow cytometer (for the silica particles). Consequently, the absolute fluorescence values could not be directly compared. The signal originating from light scattering was subtracted from the data (particles with adsorbed membrane, but without any fluorophores). The errors in these numbers are <10%. [b]Data from ref 29.

The fluorescence from the CytcO-vesicle solution containing (i) fluorescent lipids was ~10 times larger than from that containing (ii) fluorescein-labeled CytcO (Table 1). Each CytcO binds approximately one fluorescein molecule per enzyme[30] and the vesicle−CytcO ratio was approximately unity. The number of lipid molecules per vesicle was ~5000 (diameter ≅ 25 nm) and the Fluo-DOPE (fluorescent lipid) mole fraction was ~0.07%, which yields an average of ~3.5 such lipids per vesicle. In other words, the ratio of fluorophores in vesicles containing Fluo-DOPE and fluorescein-labeled CytcO was ~3.5. The larger observed fluorescence ratio of ~10 is explained by a fraction (~50%) of vesicles without protein in the sample containing fluorescein-labeled CytcO (not all CytcO molecules are reconstituted into the membrane, see Methods section).

For comparison, Table 1 also includes data from our recent study[29] on adsorption of vesicles, loaded with water-soluble fluorescein, to silica particle surfaces (see iii). As seen in the table the relative fluorescence originating from the entrapped fluorescein was much larger for the vesicles prior to than after interaction with the silica particles, which indicates that the vesicles break upon interaction with the particles (see more detailed discussion in ref 29).

To examine whether a continuous membrane-CytcO layer covering the entire surface of the particle was formed (as compared to isolated patches covering only part of the surface), we tested if the interior of the particle was isolated from the surrounding water solution. In the case of CytcO such a test can be done by studying the turnover activity of the enzyme itself without the need of adding, for example, additional dye molecules. As outlined above in the introduction section, this activity involves electron transfer from the electron donor, cytochrome *c*, which binds on the positive side of the protein, to the catalytic site, located in the interior of the protein closer to the negative side. The electron transfer is accompanied by proton uptake from the negative side to the catalytic site, where O_2 is eventually reduced to H_2O, that is, the overall reaction is equivalent to moving a positive charge from the negative to the positive side, across the membrane. Furthermore, CytcO pumps one proton per electron in the same direction, where both proton pumping and the proton−electron transfer to the catalytic site result in built-up of a transmembrane electrochemical proton gradient. Upon formation of this gradient the turnover activity of the CytcO decreases. If proton and potassium ionophores are added the electrochemical gradient collapses and the activity increases again. The ratio of the rates in the presence of the ionophores and in their absence (*i.e.*, the ratio of the slopes after and before addition of ionophores) is referred to as the "respiratory control ratio" (RCR), which is a measure of the tightness of the lipid membrane. Values >1 indicate that the membrane slows down diffusion of protons back into the

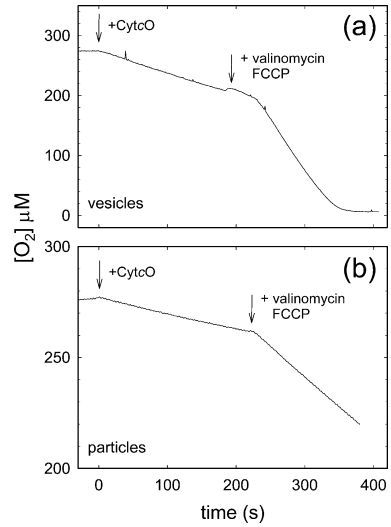

Figure 2. Activity and respiratory-control ratio (RCR). The O_2-consumption activity of Cyt*c*O vesicles (a) and Cyt*c*O-membrane-covered particles (b) before and after addition of ionophores. The ratio of the activities with and without ionophores is the respiratory-control ratio (RCR), which is a measure of proton leaks across the membrane. RCR values of ~4 and ~2.7 were obtained for Cyt*c*O-containing vesicles and particles, respectively. In both plots a and b all O_2 was consumed (*i.e.*, final O_2 concentration = 0), but due to the slower O_2-consumption rate (due to lower Cyt*c*O concentration in the particle than in the vesicle sample, see also text for explanation) plot b is interrupted at $t = 400$ s. Experimental conditions: 100 mM KCl, 25 mM HEPES at pH 7.4, 6 mM ascorbate, 70 nM TMPD, and 30 μM oxidized cytochrome *c*. At time = 0, 10 μL of a Cyt*c*O-vesicle solution (a) or 20 μL of a Cyt*c*O-membrane-particle solution (b) (see Methods section) was added (gives ~10 times higher Cyt*c*O concentration in panel a than in panel b) and the O_2-consumption rate was monitored. Then 3 μL of 2 mM valinomycin (K^+ ionophore) and 3 μL of 10 mM FCCP (carbonyl cyanide-*p*-trifluoromethoxyphenylhydrazone) (H^+ ionophore) were added as indicated in the figure.

particles such that a transmembrane electrochemical potential develops, which diminishes the Cyt*c*O activity. It should be noted that an RCR of >1 would also be obtained if intact Cyt*c*O-vesicles were adsorbed at the surface of the silica particles. We exclude this possibility based on the observation that the vesicles break upon interaction with the surface of the silica particles.[29]

Figure 2 shows O_2-consumption as a function of time for the Cyt*c*O-vesicles alone and for Cyt*c*O-vesicles deposited on the particle surface. The slope (*cf.*, O_2-consumption rate) corresponding to the fully uncoupled system (*i.e.*, after the addition of ionophores, which directly reflects the Cyt*c*O activity) was ~7 times larger for the vesicle than for the particle sample (note the different ordinate scales). This difference in slopes is consistent with the factor of ~10 lower Cyt*c*O concentration in the latter sample, which indicates that the Cyt*c*Os incorporated into the lipid bilayers supported onto the particle surface are fully active. For the Cyt*c*O-containing vesicles the RCR was 4.0 ± 0.3 (standard error (SE), 3 measurements). For the Cyt*c*O-containing membrane-covered silica particles the RCR value was 2.7 ± 0.6 (SE, 5 measurements). The lower value measured with the Cyt*c*O-containing membrane supported onto the particles as compared to the vesicles alone is reasonable considering that the surface area of the particles is ~500 ($r_{particle}^2/r_{vesicle}^2 = 275^2/12.5^2$) times larger than that of the vesicles. Here we assume that the leakage rate increases with increasing membrane surface area. It should also be noted that the experiment is sensitive to proton leaks, which presumably occur due to dynamic fluctuations of the membrane and not through "holes" across the membrane (which would allow protons to move freely across the membrane yielding an RCR of unity). Thus, even though there is a spread in the RCR values, the fact that values of >1 are observed for the particles shows that the interior was insulated from the exterior by an intact membrane. In other words, the entire particles were covered by a membrane. In addition, these results also show that the Cyt*c*O adsorbed to the particle surface is functional, not only when considering O_2-reduction catalysis, but also when considering charge separation across the membrane.

Another approach to study the integrity of the catalytic site of Cyt*c*O incorporated into the particle-supported membrane (which reflects the integrity of the entire protein) is to examine ligand binding to the site. When Cyt*c*O is reduced under anaerobic conditions in the presence of carbon monoxide, heme a_3 binds the CO ligand. The iron-CO bond is photolabile and, consequently, the CO ligand can be fully dissociated from Cyt*c*O by means of a short laser flash. When studied in detergent solution, after dissociation, the CO ligand then recombines with a rate constant of ~10 ms at 1 mM CO (saturated CO solution)[31] As seen in Figure 3 (compare any of the traces in panel a to those in panel b, see further explanation later) the CO-recombination time constant was about the same for the particle-supported membrane-bound Cyt*c*O as for Cyt*c*O in lipid vesicles or in detergent solution, which also indicates an intact catalytic site.

The orientation of Cyt*c*O in the vesicles was determined by selectively reducing the enzyme from different sides of the membrane. First, Cyt*c*O was reduced with a membrane-impermeable reducing agent (hexamineruthenium chloride, analogue of cytochrome *c*), which reduces only Cyt*c*O with the cytochrome *c*-binding site facing the outside (positive side) solution ("correctly" oriented Cyt*c*O). Then, another reducing agent (dithionite), which can reduce also the "incorrectly" oriented population, was added. The fraction of reduced Cyt*c*O after the additions is typically determined from measurements of the optical absorption spectra. However, this approach was found to be inaccurate when used to determine the orientation of Cyt*c*O in the membranes deposited at the silica particle surfaces due to significant light scattering of the particles. To circumvent this problem we instead used an ap-

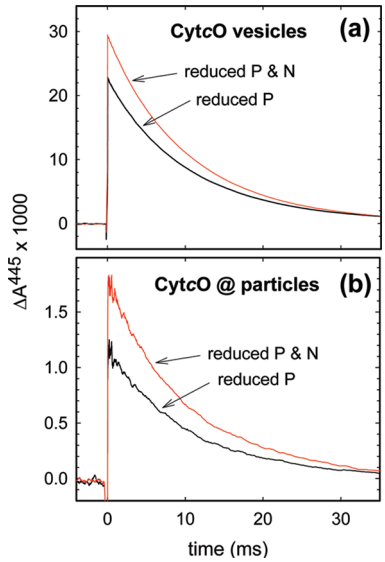

Figure 3. Flash photolysis of the Cytc*O*-carbon monoxide complex. Measurements were done with the Cytc*O*-vesicles (a) and with Cytc*O*-containing membrane deposited on silica particles (b). A laser flash at time = 0 dissociated the Cytc*O*−CO complex, which is seen as an absorbance increase at 445 nm. The decrease in absorbance is associated with rebinding of CO to heme a_3. The absorbance change at time = 0 is a measure of the amount of reduced Cytc*O* because only reduced heme a_3 binds CO. The lower traces in panels a and b were obtained after reduction of Cytc*O* exclusively from the positive (P) side of the membrane side and the upper traces after reduction of the whole population (P and N sides). Experimental conditions: 100 mM KCl, 25 mM HEPES at pH 7.4, 2 mM ascorbate, 2 μM hexammineruthenium chloride, [CO] ≅ 1 mM, T = 22 °C. Dithionite was added for full reduction of Cytc*O*.

proach based on measurements of differences in absorbance after flash photolysis of the CO ligand from reduced Cytc*O* as described above (Figure 3). In these experiments the CO-dissociation amplitude at time = 0 is a measure of the amount reduced Cytc*O* because the CO ligand binds exclusively to the reduced form of heme a_3. The advantage of using this approach is that differences in absorbance are measured at the time of the laser flash (CO photolysis) rather then the absolute absorption spectrum of the Cytc*O*. Consequently, the background "absorbance" (*cf.* scattering) is less of a problem. Figure 3a shows flash-induced absorbance changes of the Cytc*O*-containing vesicles after addition of a membrane-impermeable (reduces only the "correctly oriented" Cytc*O*, *i.e.*, from the positive side, "reduced P") and membrane-permeable (reduces Cytc*O* from both sides, "reduced P & N") reducing agent. The orientation was determined, from the ratio of the amplitudes at zero time, to be 71 ± 4% (SE, n = 5) "correctly oriented" Cytc*O*. After deposition of the membrane at particles we obtained a ratio of 68 ± 5% (SE, n = 10), which shows that the orientation is maintained during the coverage process. In a recent study it was observed that ~70% of bacteriorhodopsin molecules were correctly oriented when incorporated into mesoporous microspheres-supported-bilayer membranes even though the bacteriorhodopsin was initially oriented unidirectionally in the predeposited vesicles.[23] It was proposed that upon interaction of the bacteriorhodopsin-containing membrane with the silica particle surface two transient bacteriorhodopsin-membrane populations were formed, which eventually adsorb onto the surface resulting in the observed orientation.[23] In our study the Cytc*O* orientation was preserved during breaking of the Cytc*O*-vesicles and deposition of the Cytc*O*-membrane onto the particle surface (Figure 4), which is consistent with a study of adsorption of lipid vesicles containing the Tissue Factor transmembrane protein to the inner surface of glass microcapillaries.[32]

The ratio of the maximum amplitudes (see Figure 3, both populations reduced) obtained with Cytc*O*-containing vesicles only and the Cytc*O*-membrane-particle system was 15 ± 1 (SE, n = 10). This ratio can also be estimated by comparison of the amount of Cytc*O* in the vesicle solution and the amount of Cytc*O*

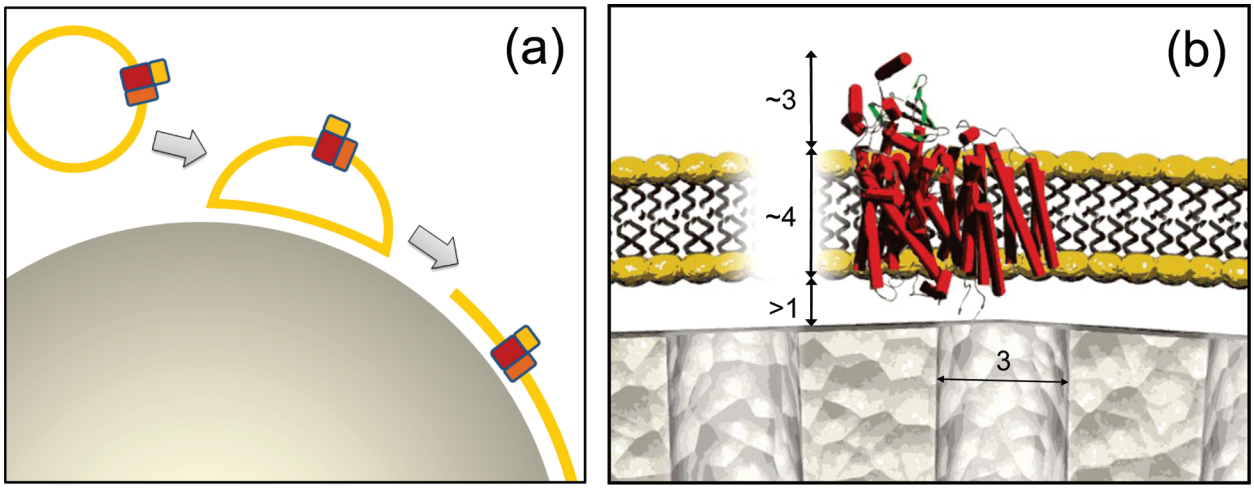

Figure 4. Schematic cartoon summarizing the data. (a) The adsorption process is illustrated showing the interaction of the Cytc*O*-containing vesicles with the particle surface. The orientation of the Cytc*O* is preserved during adsorption. (b) Schematic illustration of membrane-Cytc*O*-particle system. The numbers show approximate distances in nm. Note that the picture is not drawn to scale.

added from that solution to the particle suspension. If all vesicles added to the particle suspension were adsorbed at the particle outer surface, then we would expect an amplitude ratio equal to the ratio of the total vesicle and the total particle outer surface area (A_V/A_P), which was 27 ± 1 (SE, $n = 10$). If part of the Cyt*c*O population would be "deactivated" due to interactions with the silica colloids then we would expect a CO-dissociation amplitude ratio of >27. The observation of a ratio that is <27 indicates that CO binding is not perturbed by interactions with the silica particles. In addition, the observation of two active Cyt*c*O populations (which are the same as in the lipid vesicles) with different orientations in the silica-supported membrane also indicates that none of the orientations is disproportionally deactivated.

As described in the Methods section the particles with fluorescein-labeled Cyt*c*O in the membrane were washed several times such that the original Cyt*c*O-vesicle solution was diluted by a factor of $\sim 10^{-8}$. Thus, the observed ratio of the absorbance changes of ~15 shows that the Cyt*c*O molecules were associated with the mesoporous particles and not free vesicles.

The results are consistent with other data showing that upon deposition of membranes on silica surfaces containing nm-sized pores, the membrane is able to span across the pore openings rather then penetrating into the pores[33] (Figure 4). In addition, it has also been shown that there is a water-filled space between a lipid membrane and a (dense) silica surface that may be ~10 Å thick.[34−36] We speculate that the porous nature of the exterior surface of the mesoporous spheres also could contribute to a thicker fluid film between the membrane and the solid support because of the decrease in the attractive van der Waals interaction between the lipids and the water−silica composite surface. In this context we note that, as discussed above, Cyt*c*O turnover requires proton uptake from the negative side of the membrane, which requires a water-filled space on the inside of the membrane. With the mesoporous structure the accessible volume on the inside of the membrane is defined by the surface water film as well as the entire pore volume; therefore, the inside volume is significantly larger than that of a solid silica particle. In future studies a more uniform orientation of Cyt*c*O could be achieved by chemically modifying the silica surface to allow specific interactions with, for example, a histidine tag as has been done previously for planar gold surfaces.[24−27]

In summary, the results described above show that the mesoporous silica particles were entirely covered by defect-free membranes containing the multisubunit, redox-driven proton pump, Cyt*c*O. The incorporated enzymes remained active, both with respect to catalysis of reduction of O_2 to H_2O and transmembrane charge separation. The use of mesoporous silica particles may be beneficial to obtain supported lipid bilayers with a large interspace that is sufficient to provide a proton source and also connect the water space around the Cyt*c*O negative side surface with the entire volume of the particle through the pores. This supramolecular architecture with an inner pore structure mimicking a cytoskeleton yields a solid-supported biofunctional cellular surface, which provides a basis for functional studies of membrane-bound transport proteins, and also for applications within pharmaceutical drug delivery.

METHODS

Synthesis of the Monodisperse Mesoporous Colloids. Mesostructured silica spheres were synthesized from dilute solutions of the cationic surfactant, hexadecyltrimethylammonium bromide (C_{16}TAB), in an alkaline/methanol/water solution that contains hydrolyzed tetramethylorthosilicate (TMOS) following a previously published procedure.[28] The as-synthesized particles were thermally calcined at 550 °C, at a ramp rate of 1 °C per minute, for 5 h in air. The morphology of the particles was determined using scanning electron microscopy, JEOL 820 SEM, operating at 8−10 keV. The particles were thinly spread onto a carbon film supported on a brass stud and gold coated. The XRD patterns were obtained using a XPERT-PRO powder diffractometer (Cu Kα radiation, $k = 1.5418$ Å) over the range of $2\theta = 1.0-10.0°$. Porosity measurements were performed volumetrically using a Micromeritics ASAP 2020 analyzer. The particles were degassed at 150 °C for 10 h and data collection started typically at −196 °C, following a program consisting of both an adsorption and desorption branch. The specific surface areas, S_{BET} ($m^2\ g^{-1}$) were calculated using the Brunauer− Emmett−Teller (BET) model within the 0.05−0.15 $p/p°$ relative pressure region.[37] The pore volume, V_{pore} ($cm^3\ g^{-1}$), was estimated from the amount of N_2-adsorbed at a relative pressure around $P/P_0 = 0.99$. The pore size distribution was calculated based on the NLDFT (nonlocal density functional theory)[38] method, and the mesopore size, $Ø_{pore}$ (nm), was determined from the maximum of the pore size distribution curve. Transmission electron microscopy (TEM) micrographs of thin microtomed slices of the calcined particles were obtained using a JEOL JEM-3010 microscope operating at an accelerating voltage of 300 keV equipped with a CCD camera (model Keen View, SIS analysis) (for details, see ref 28).

Purification of Cyt*c*O. The *R. sphaeroides* bacteria were grown aerobically in shake incubators at 30 °C. The cells were harvested and the His-tagged Cyt*c*O was purified as described previously.[39] It consists of four subunits with a total molecular weight of ~100 kDa (for discussion of the structure and function of Cyt*c*O, see refs 40−44). The enzyme was frozen in liquid nitrogen and stored in 0.1 M Hepes-KOH, pH 7.4, 0.1% dodecyl β-D-maltoside in a −80 °C freezer.

Reconstitution of Cyt*c*O into Lipid Vesicles. The lipids 1,2-dioleoyl-*sn*-glycero-3-phosphoethanolamine (DOPE), 1,2-dioleoyl-*sn*-glycero-3-phosphocholine (DOPC), 1,2-dioleoyl-*sn*-glycero-3-[phospho-*rac*-(1-glycerol)] (DOPG) and 1,1′2,2′-tetraoleoyl cardiolipin (CA) (all from Avanti Polar Lipids Inc.) were dissolved in chloroform and methanol (2:1 volume ratio) and then dried under continuous flow of nitrogen during ~30 min. The lipid mixture at a weight ratio of 9:6:4:1 of DOPE:DOPC:DOPG:CA was suspended, at a total lipid concentration of 6 mg/mL, in a solution of 100 mM KCl, 25 mM HEPES pH 7.4. This lipid mixture was chosen to approximately mimic those of *Escherichia coli* and *R. sphaeroides* (source of the Cyt*c*O in our experiments). In experiments where the fluorescein-labeled lipids (1,2-dioleoyl-*sn*-

glycero-3-phosphoethanolamine-*N*-(carboxyfluorescein) (Fluo-DOPE)), were used, the weight ratio of the lipids mixture DOPE:DOPC:DOPG:CA:Fluo-DOPE was 9:6:4:1:0.02. This mixture gives a Fluo-DOPE mole fraction of 0.07%. The lipid solutions were sonicated (Heat Systems Sonicator XL) in 30 s on/off cycles for a total of 10 min to form small unilamellar vesicles.

Reconstitution of CytcO was performed following published procedures.[44,45] In short the sonicated lipids, supplemented with 0.3% cholate, were mixed at a 1:1 volume ratio with 2.4 μM CytcO in 0.6% cholate, 100 mM KCl, and 25 mM HEPES at pH 7.4. The detergent was then removed by addition of Bio-Beads (see ref 45). The CytcO and vesicle concentrations were chosen such that the CytcO/vesicle ratio was approximately unity, that is, one CytcO per vesicle. However, not all enzyme molecules were reconstituted into the membrane and a fraction of the vesicles remained empty (Faxén *et al*., unpublished data). The diameter of the vesicles was estimated to be 25 ± 5 nm using dynamic light-scattering (Nano Z, Malvern Instruments). The CytcO-vesicle solution (~0.5 μM CytcO) was transferred to a sealed cuvette and the atmosphere was exchanged to nitrogen on a vacuum line. The CytcO was then reduced by adding 2 mM ascorbate, 2 μM hexammineruthenium chloride and then the N_2 atmosphere was exchanged for CO. Formation of the CytcO−CO complex was verified using the optical absorption spectrum.

Formation of Supported Lipid Bilayers on Mesoporous Silica Particles. Mesoporous silica particles at a concentration of 5 mg/mL were suspended in an electrolyte buffer solution that contained 100 mM KCl, 25 mM HEPES at pH 7.4 and were sonicated to remove any aggregates. The particle suspension was then mixed for 1 h at room temperature with the lipid vesicles, with or without reconstituted CytcO. The total volume of the mixture was 2 mL and the ratio between the total vesicle and the total particle outer surface area (A_V/A_P) was 25−30 (the A_V/A_P ratio was calculated as described in ref 29). The number of lipids (*cf.* vesicle concentration) was determined from the total amount of phosphorus.[29,46] After mixing, a buffer solution of 100 mM KCl, 25 mM HEPES pH 7.4 was added to make a final volume of 10 mL, and the mixture was centrifuged at 720*g* for 15 min. The resulting particle pellet had an approximate volume of 200 μL. The supernatant containing superfluous vesicles was discarded and the pellet was resuspended in 10 mL buffer solution. The centrifugation procedure was repeated two times, and the final pellet was solubilized in 1 mL of a solution of 100 mM KCl, 25 mM HEPES pH 7.4. After this treatment the concentration of the free vesicles in solution was estimated to be $\sim 10^{-6}$ % of the initial amount added.

Analysis of the CytcO-Membrane Covered Particles. The fluorescence of different types of CytcO-containing vesicles: (i) with fluorescent lipids added, (ii) with maleimide-fluorescein-labeled CytcO (the labeling procedure is described in ref 30) (no fluorescent lipids), and (iii) with fluorescein trapped within the vesicles was measured using a fluorometer (Varian Cary Eclipse). Four different types of CytcO-containing membrane covered particles were prepared and analyzed using flow cytometry (BD FACSCalibur with BD FACSFlow Sheath Fluid as liquid vector (BD Biosciences, Canada)): type i−iii as described above, and (iv) no fluorophores added (used to determine the background "fluorescence" signal originating from light scattering).

Measurements of CytcO Activity. The CytcO activity at 22°C was determined by measuring the O_2-consumption rate using an oxygraph (Hansatech Instruments Ltd., UK). The background (non-enzymatically catalyzed) O_2-consumption rate was first determined after adding 1.5 mL of a solution composed of 100 mM KCl, 25 mM HEPES at pH 7.4, 6 mM ascorbate, 70 nM *N,N,N′,N′*-tetramethyl-*p*-phenylenediamine (TMPD) and 30 μM oxidized cytochrome *c*. Then, 10 μL of a solution with CytcO-containing vesicles (see earlier) or 20 μL of a suspension of particle-supported CytcO-membrane (see earlier) was added and the O_2-consumption rate was monitored. The activity was determined from the difference in the slopes after and before the CytcO addition. To determine the CytcO activity in the absence of a proton electrochemical gradient, 3 μL of a 2 mM (4 μM final concentration) valinomycin solution (K^+ ionophore) and 3 μL of a 10 mM (20 μM final concentration) FCCP (carbonyl cyanide-*p*-trifluoromethoxyphenylhydrazone) solution (H^+ ionophore) were added.

Laser Flash Photolysis. The CO ligand was dissociated from CytcO using an 8 ns laser pulse with an energy of ~100 mJ at 532 nm (Nd:YAG Quantel Brilliant B, Les Ulis Cedex, France). Time-resolved optical absorbance changes were recorded using a flash photolysis setup from Applied Photophysics (model LKS.60, Surrey, UK)). The cuvette path length was 1.00 cm. Monochromators both in front and after the cuvette were used to select the appropriate wavelength.

Acknowledgment. The project was supported by funding from the Center for Biomembrane Research at Stockholm University and the Knut and Alice Wallenberg Foundation.

REFERENCES AND NOTES

1. Kresge, C. T.; Leonowicz, M. E.; Roth, W. J.; Vartuli, J. C.; Beck, J. S. Ordered Mesoporous Molecular Sieves Synthesized by a Liquid-Crystal Template Mechanism. *Nature* **1992**, *359*, 710–712.
2. Che, S.; Li, H.; Lim, S.; Sakamoto, Y.; Terasaki, O.; Tatsumi, T. Synthesis Mechanism of Cationic Surfactant Templating Mesoporous Silica under an Acidic Synthesis Process. *Chem. Mater.* **2005**, *17*, 4103–4113.
3. Rama Rao, G. V.; López, G. P.; Bravo, J.; Pham, H.; Datye, A. K.; Xu, H. F.; Ward, T. L. Monodisperse Mesoporous Silica Microspheres Formed by Evaporation-Induced Self Assembly of Surfactant Templates in Aerosols. *Adv. Mater.* **2002**, *14*, 1301–1304.
4. Rathousky, J.; Zukalov, M.; Zukal, A.; Had, J. Homogeneous Precipitation of Siliceous Mcm-41 and Bimodal Silica. *Collect. Czech. Chem. Commun.* **1998**, *63*, 1893–1906.
5. Yang, H.; Coombs, N.; Ozin, G. A. Morphogenesis of Shapes and Surface Patterns in Mesoporous Silica. *Nature* **1997**, *386*, 692–695.
6. Slowing, I. I.; Vivero-Escoto, J. L.; Wu, C. W.; Lin, V. S. Y. Mesoporous Silica Nanoparticles as Controlled Release Drug Delivery and Gene Transfection Carriers. *Adv. Drug Delivery Rev.* **2008**, *60*, 1278–1288.
7. Lai, C. Y.; Trewyn, B. G.; Jeftinija, D. M.; Jeftinija, K.; Xu, S.; Jeftinija, S.; Lin, V. S. Y. A Mesoporous Silica Nanosphere-Based Carrier System with Chemically Removable Cds Nanoparticle Caps for Stimuli-Responsive Controlled Release of Neurotransmitters and Drug Molecules. *J. Am. Chem. Soc.* **2003**, *125*, 4451–4459.
8. Salonen, J.; Laitinen, L.; Kaukonen, A. M.; Tuura, J.; Björkqvist, M.; Heikkilä, T.; Vähä-Heikkilä, K.; Hirvonen, J.; Lehto, V. P. Mesoporous Silicon Microparticles for Oral Drug Delivery: Loading and Release of Five Model Drugs. *J. Controlled Release* **2005**, *108*, 362–374.
9. Wu, E. C.; Park, J. H.; Park, J.; Segal, E.; Cunin, F.; Sailor, M. J. Oxidation-Triggered Release of Fluorescent Molecules or Drugs from Mesoporous Si Microparticles. *ACS Nano* **2008**, *2*, 2401–2409.
10. Liong, M.; Lu, J.; Kovochich, M.; Xia, T.; Ruehm, S. G.; Nel, A. E.; Tamanoi, F.; Zink, J. I. Multifunctional Inorganic Nanoparticles for Imaging, Targeting, and Drug Delivery. *ACS Nano* **2008**, *2*, 889–896.
11. Lu, J.; Liong, M.; Zink, J. I.; Tamanoi, F. Mesoporous Silica Nanoparticles as a Delivery System for Hydrophobic Anticancer Drugs. *Small* **2007**, *3*, 1341–1346.
12. Hernandez, R.; Tseng, H. R.; Wong, J. W.; Stoddart, J. F.; Zink, J. I. An Operational Supramolecular Nanovalve. *J. Am. Chem. Soc.* **2004**, *126*, 3370–3371.
13. Mal, N. K.; Fujiwara, M.; Tanaka, Y. Photocontrolled Reversible Release of Guest Molecules from Coumarin-Modified Mesoporous Silica. *Nature* **2003**, *421*, 350–353.
14. Nguyen, T. D.; Tseng, H. R.; Celestre, P. C.; Flood, A. H.; Liu, Y.; Stoddart, J. F.; Zink, J. I. A Reversible Molecular Valve. *Proc. Natl. Acad. Sci. U.S.A.* **2005**, *102*, 10029–10034.
15. Loidl-Stahlhofen, A.; Schmitt, J.; Nöller, J.; Hartmann, T.; Brodowsky, H.; Schmitt, W.; Keldenich, J., Solid-Supported Biomolecules on Modified Silica Surfaces—A Tool for Fast Physicochemical Characterization and High-Throughput Screening. Adv. Mater. **2001**, *13*.

16. Katagiri, K.; Hashizume, M.; Kikuchi, J. I.; Taketani, Y.; Murakami, M. Creation of Asymmetric Bilayer Membrane on Monodispersed Colloidal Silica Particles. *Colloids Surf., B* **2004**, *38*, 149–153.
17. Baksh, M. M.; Jaros, M.; Groves, J. T. Detection of Molecular Interactions at Membrane Surfaces through Colloid Phase Transitions. *Nature* **2004**, *427*, 139–141.
18. Moura, S. P.; Carmona-Ribeiro, A. M. Biomimetic Particles: Optimization of Phospholipid Bilayer Coverage on Silica and Colloid Stabilization. *Langmuir* **2005**, *21*, 10160–10164.
19. Moura, S. P.; Carmona-Ribeiro, A. M. Cationic Bilayer Fragments on Silica at Low Ionic Strength: Competitive Adsorption and Colloid Stability. *Langmuir* **2003**, *19*, 6664–6667.
20. Trepout, S.; Mornet, S.; Benabdelhak, H.; Ducruix, A.; Brisson, A. R.; Lambert, O. Membrane Protein Selectively Oriented on Solid Support and Reconstituted into a Lipid Membrane. *Langmuir* **2007**, *23*, 2647–54.
21. Mornet, S.; Lambert, O.; Duguet, E.; Brisson, A. The Formation of Supported Lipid Bilayers on Silica Nanoparticles Revealed by Cryoelectron Microscopy. *Nano Lett.* **2005**, *5*, 281–285.
22. Liu, J.; Stace-Naughton, A.; Jiang, X.; Brinker, C. J. Porous Nanoparticle Supported Lipid Bilayers (Protocells) as Delivery Vehicles. *J. Am. Chem. Soc.* **2009**, *131*, 1354–1355.
23. Davis, R. W.; Flores, A.; Barrick, T. A.; Cox, J. M.; Brozik, S. M.; Lopez, G. P.; Brozik, J. A. Nanoporous Microbead Supported Bilayers: Stability, Physical Characterization, and Incorporation of Functional Transmembrane Proteins. *Langmuir* **2007**, *23*, 3864–3872.
24. Friedrich, M. G.; Plum, M. A.; Santonicola, M. G.; Kirste, V. U.; Knoll, W.; Ludwig, B.; Naumann, R. L. C. *In Situ* Monitoring of the Catalytic Activity of Cytochrome *c* Oxidase in a Biomimetic Architecture. *Biophys. J.* **2008**, *95*, 1500–1510.
25. Ataka, K.; Richter, B.; Heberle, J. Orientational Control of the Physiological Reaction of Cytochrome *c* Oxidase Tethered to a Gold Electrode. *J. Phys. Chem. B* **2006**, *110*, 9339–9347.
26. Ataka, K.; Giess, F.; Knoll, W.; Naumann, R.; Haber-Pohlmeier, S.; Richter, B.; Heberle, J. Oriented Attachment and Membrane Reconstitution of His-Tagged Cytochrome *c* Oxidase to a Gold Electrode: In Situ Monitoring by Surface-Enhanced Infrared Absorption Spectroscopy. *J. Am. Chem. Soc.* **2004**, *126*, 16199–16206.
27. Giess, F.; Friedrich, M. G.; Heberle, J.; Naumann, R. L.; Knoll, W. The Protein-Tethered Lipid Bilayer: A Novel Mimic of the Biological Membrane. *Biophys. J.* **2004**, *87*, 3213–3220.
28. Ng, J. B. S.; Vasiliev, P. O.; Bergström, L. The Radial Dependence of the Spatial Mesostructure of Monodisperse Mesoporous Silica Spheres. *Microporous Mesoporous Mater.* **2008**, *112*, 589–596.
29. Nordlund, G.; Lönneborg, R.; Brzezinski, P. Formation of Supported Lipid Bilayers on Silica Particles Studied Using Flow Cytometry. *Langmuir* **2009**, *25*, 4601–6.
30. Öjemyr, L.; Sanden, T.; Widengren, J.; Brzezinski, P. Lateral Proton Transfer between the Membrane and a Membrane Protein. *Biochemistry* **2009**, *48*, 2173–2179.
31. Ädelroth, P.; Brzezinski, P.; Malmström, B. G. Internal Electron Transfer in Cytochrome *c* Oxidase from Rhodobacter Sphaeroides. *Biochemistry* **1995**, *34*, 2844–2849.
32. Contino, P. B.; Hasselbacher, C. A.; Ross, J. B. A.; Nemerson, Y. Use of an Oriented Transmembrane Protein to Probe the Assembly of a Supported Phospholipid Bilayer. *Biophys. J.* **1994**, *67*, 1113–1116.
33. Simon, A.; Girard-Egrot, A.; Sauter, F.; Pudda, C.; Picollet D'Hahan, N.; Blum, L.; Chatelain, F.; Fuchs, A. Formation and Stability of a Suspended Biomimetic Lipid Bilayer on Silicon Submicrometer-Sized Pores. *J. Colloid Interface Sci.* **2007**, *308*, 337–43.
34. Koenig, B. W.; Krueger, S.; Orts, W. J.; Majkrzak, C. F.; Berk, N. F.; Silverton, J. V.; Gawrisch, K. Neutron Reflectivity and Atomic Force Microscopy Studies of a Lipid Bilayer in Water Adsorbed to the Surface of a Silicon Single Crystal. *Langmuir* **1996**, *12*, 1343–1350.
35. Johnson, S. J.; Bayerl, T. M.; McDermott, D. C.; Adam, G. W.; Rennie, A. R.; Thomas, R. K.; Sackmann, E. Structure of an Adsorbed Dimyristoylphosphatidylcholine Bilayer Measured with Specular Reflection of Neutrons. *Biophys. J.* **1991**, *59*, 289–294.
36. Bayerl, T. M.; Bloom, M. Physical Properties of Single Phospholipid Bilayers Adsorbed to Micro Glass Beads. A New Vesicular Model System Studied by 2H-Nuclear Magnetic Resonance. *Biophys. J.* **1990**, *58*, 357–362.
37. Brunauer, S.; Emmett, P. H.; Teller, E. Adsorption of Gases in Multimolecular Layers. *J. Am. Chem. Soc.* **1938**, *60*, 309–319.
38. Ravikovitch, P. I.; Neimark, A. V. Characterization of Micro- and Mesoporosity in SBA-15 Materials from Adsorption Data by the NLDFT Method. *J. Phys. Chem. B* **2001**, *105*, 6817–6823.
39. Mitchell, D. M.; Gennis, R. B. Rapid Purification of Wildtype and Mutant Cytochrome *c* Oxidase from Rhodobacter Sphaeroides by Ni^{2+}-NTA Affinity Chromatography. *FEBS Lett.* **1995**, *368*, 148–150.
40. Brzezinski, P.; Gennis, R. B. Cytochrome *c* Oxidase: Exciting Progress and Remaining Mysteries. *J. Bioenerg. Biomembr.* **2008**, 1–11.
41. Hosler, J. P.; Ferguson-Miller, S.; Mills, D. A. Energy Transduction: Proton Transfer through the Respiratory Complexes. *Annu. Rev. Biochem.* **2006**, *75*, 165–187.
42. Wikström, M.; Verkhovsky, M. I. Towards the Mechanism of Proton Pumping by the Haem-Copper Oxidases. *Biochim. Biophys. Acta* **2006**, *1757*, 1047–1051.
43. Brzezinski, P.; Ädelroth, P. Design Principles of Proton-Pumping Haem-Copper Oxidases. *Curr. Opin. Struct. Biol.* **2006**, *16*, 465–472.
44. Faxén, K.; Gilderson, G.; Ädelroth, P.; Brzezinski, P. A Mechanistic Principle for Proton Pumping by Cytochrome *c* Oxidase. *Nature* **2005**, *437*, 286–289.
45. Jasaitis, A.; Verkhovsky, M. I.; Morgan, J. E.; Verkhovskaya, M. L.; Wikström, M. Assignment and Charge Translocation Stoichiometries of the Major Electrogenic Phases in the Reaction of Cytochrome *c* Oxidase with Dioxygen. *Biochemistry* **1999**, *38*, 2697–2706.
46. Chen, P. S.; Toribara, T. Y.; Warner, H. Microdetermination of Phosphorus. *Anal. Chem.* **1956**, *28*, 1756–1758.